Supporting Information

Rigid-soft hybrid paper-based flexible pressure sensor with ultrawide working range and frequency bandwidth

*Cong Wang[a], Jiamin Quan[a], Linpeng Liu[a,*], Peilin Cao[a], Kaiwen Ding[a], Yulong Ding[a], Xianshi Jia[a], Dejin Yan[b], Nai Lin[b] and Ji'an Duan[a]*

a State Key Laboratory of Precision Manufacturing for Extreme Service Performance,

College of Mechanical and Electrical Engineering, Central South University, Changsha
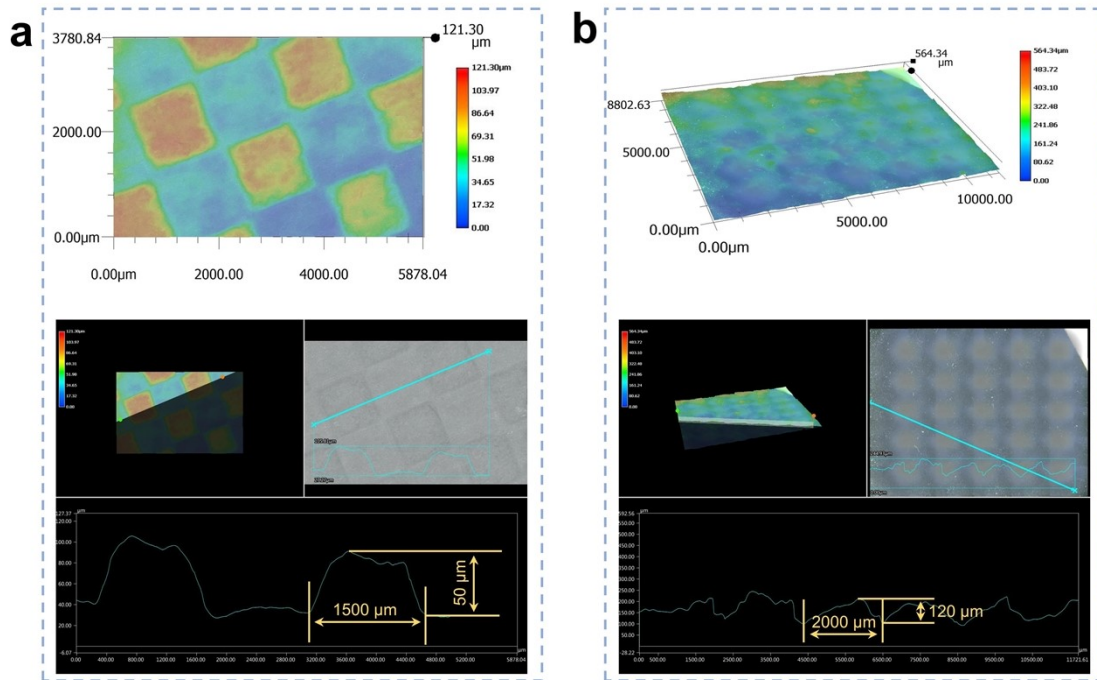
410083, China

b The 10th Research Institute of CETC, Chengdu, Sichuan 610036, China
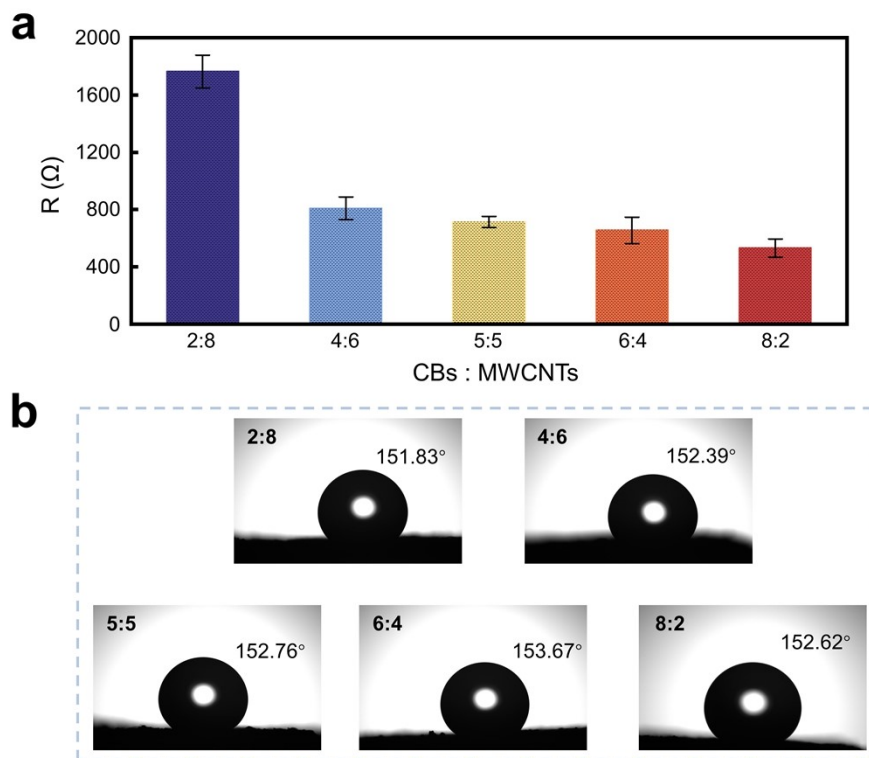
*Corresponding author: linpengliu@csu.edu.cn

Supplementary Figures
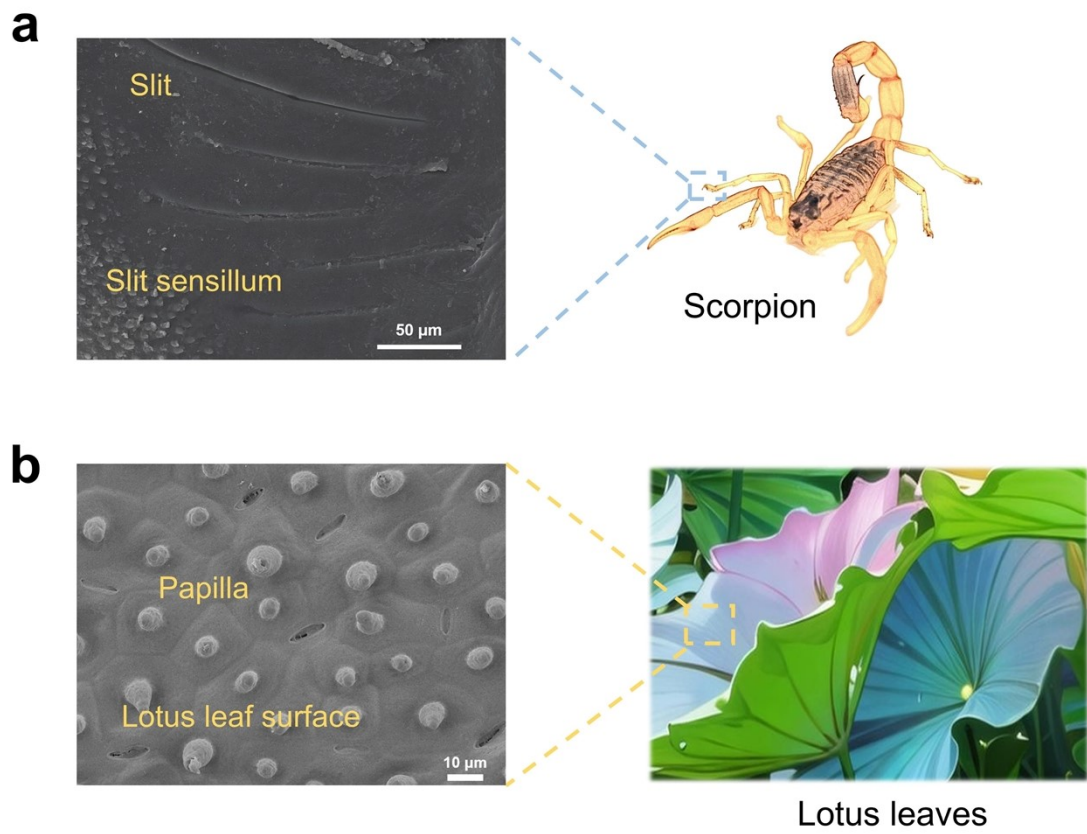
Figure S1. (a) SEM image of slit sensillum of scorpion. (b) SEM image of the surface of lotus leaf.

**Figure S2.** (a) Optical microscope image analysis of CA-paper. (b) Optical microscope image analysis of CA-paper after immersion in conductive ink.

Figure S3. (a) Resistances of the sprayed ink for different mass ratios of CBs and MWCNTs. (b) Water contact angles of the sprayed ink for different mass ratios of CBs and MWCNTs.
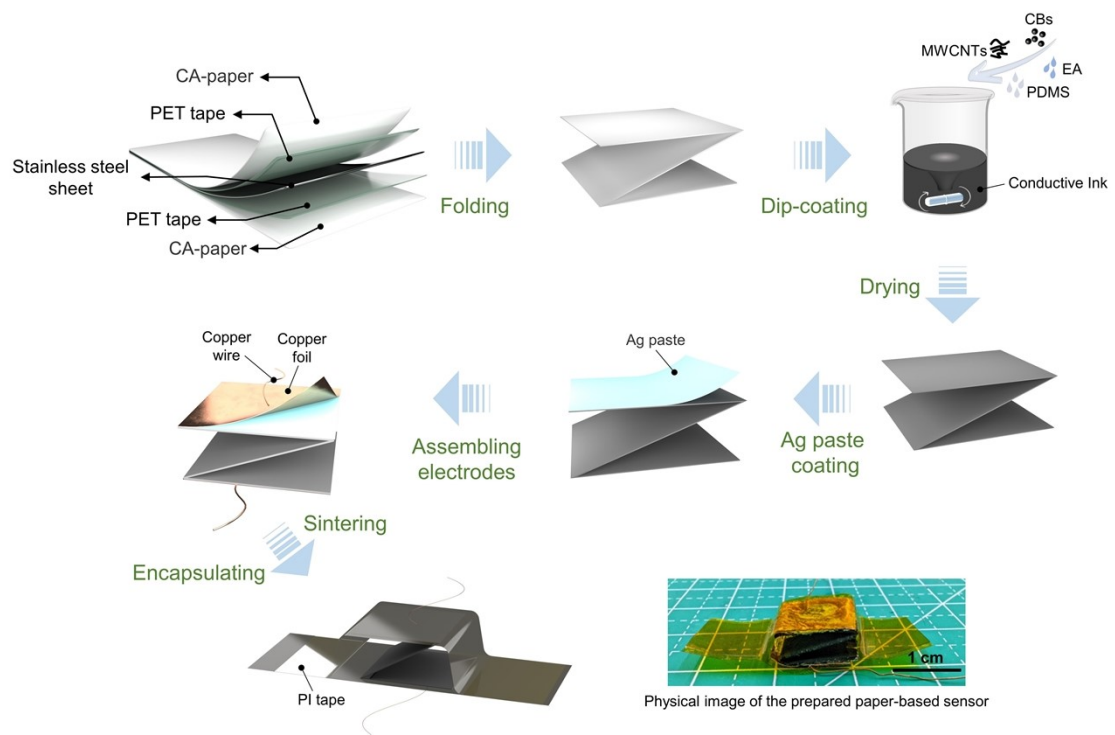
Figure S4. Schematic diagram of the preparation process of paper-based pressure sensors.
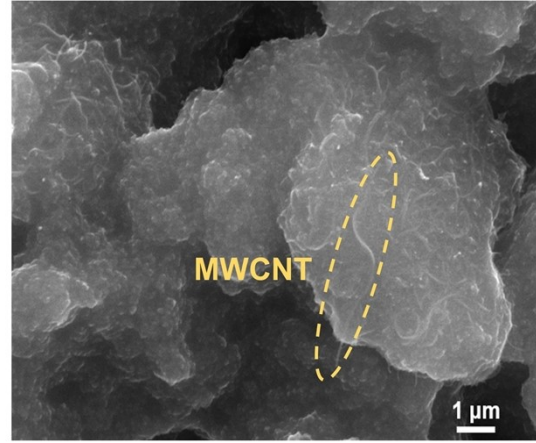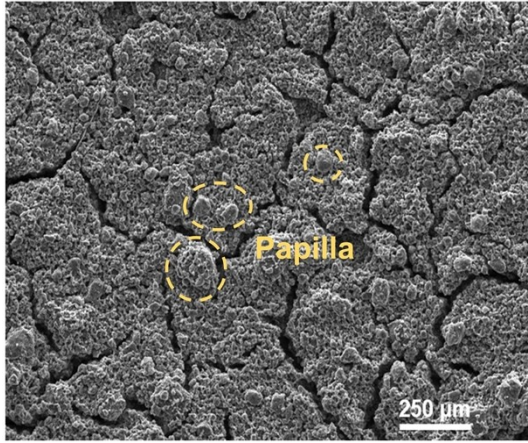
Figure S5. SEM image of MWCNTs/CBs/PDMS coating.
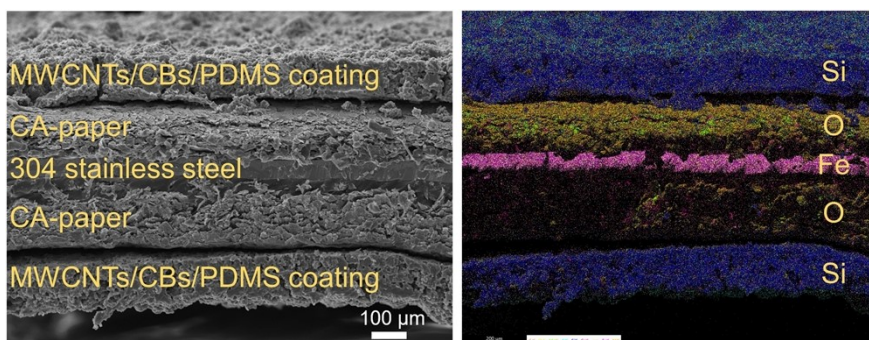
Figure S6. SEM image (left) and energy dispersive X-ray spectroscopy (EDS) analysis (right) of a single layer of the cross-section of the paper-based pressure sensor. The sensor was cut through its middle by scissors to obtain its cross-section because the steel can't be brittle fractured by flash-freezing with liquid nitrogen.
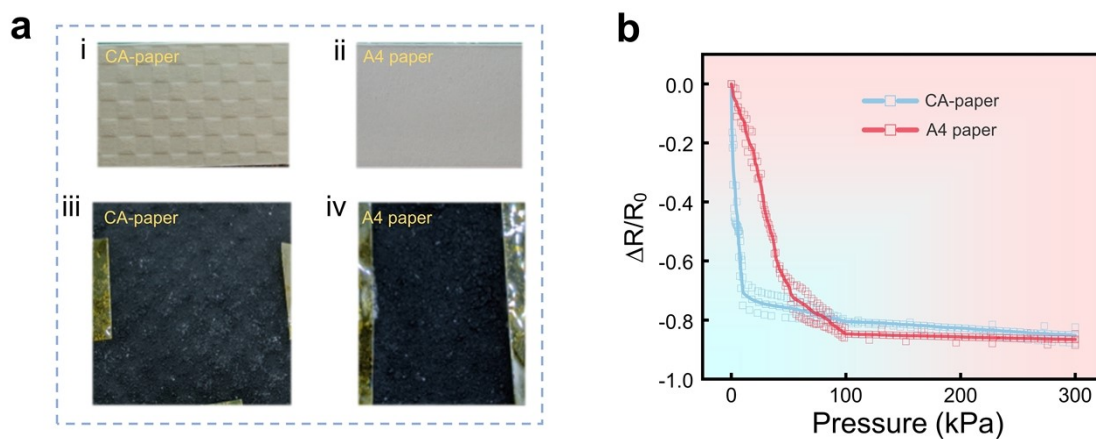
Figure S7. (a) Images of CA-paper before (i) and after (iii) immersion in conductive ink and A4 paper before (ii) and after (iv) immersion in conductive ink. (b) Pressure-Relative resistance curves for two kinds of pressure sensors (using CA-paper/A4 paper).
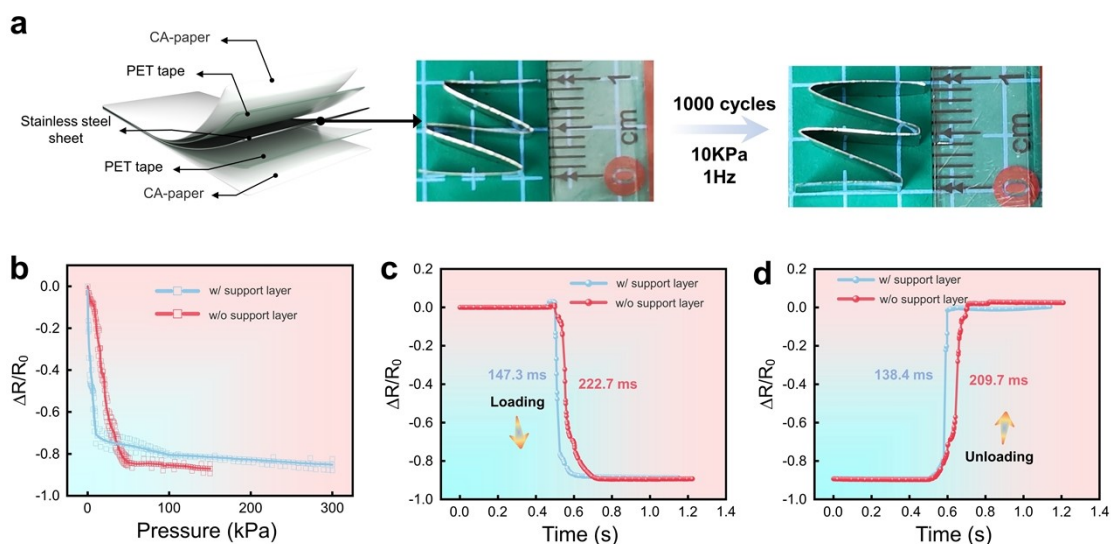
Figure S8. (a) Load/unload cyclic test of folded 304 stainless steel sheet. It can be seen that the height of the sample remained essentially unchanged before and after the cyclic test when the folded 304 stainless steel sheet was subjected to 1000 cycles at a frequency of 1 Hz under a pressure of 10 kPa. (b) Pressure-Relative resistance curves of sensors (With/Without support layer). (c) Response time of sensors (With/Without support layer) with simultaneous changes in relative resistance. (d) Recovery time of sensors (With/Without support layer) with simultaneous changes in relative resistance.
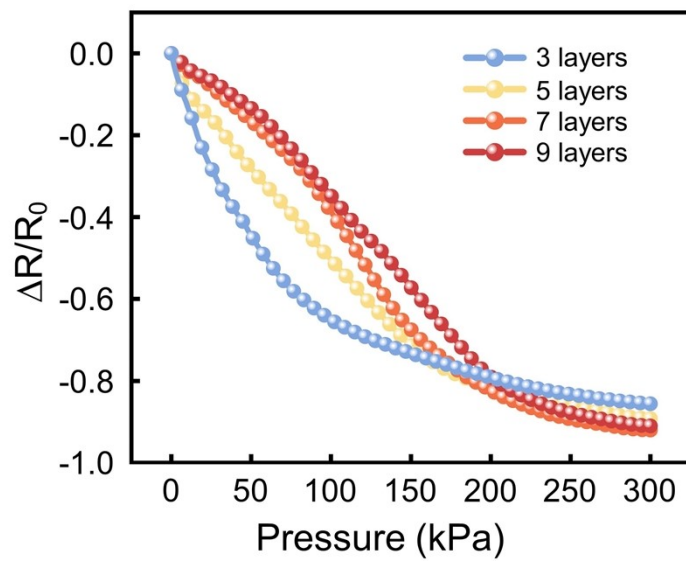
Figure S9. Relative resistance change of paper-based pressure sensors under pressure

(300 kPa) for different number of folding layers.
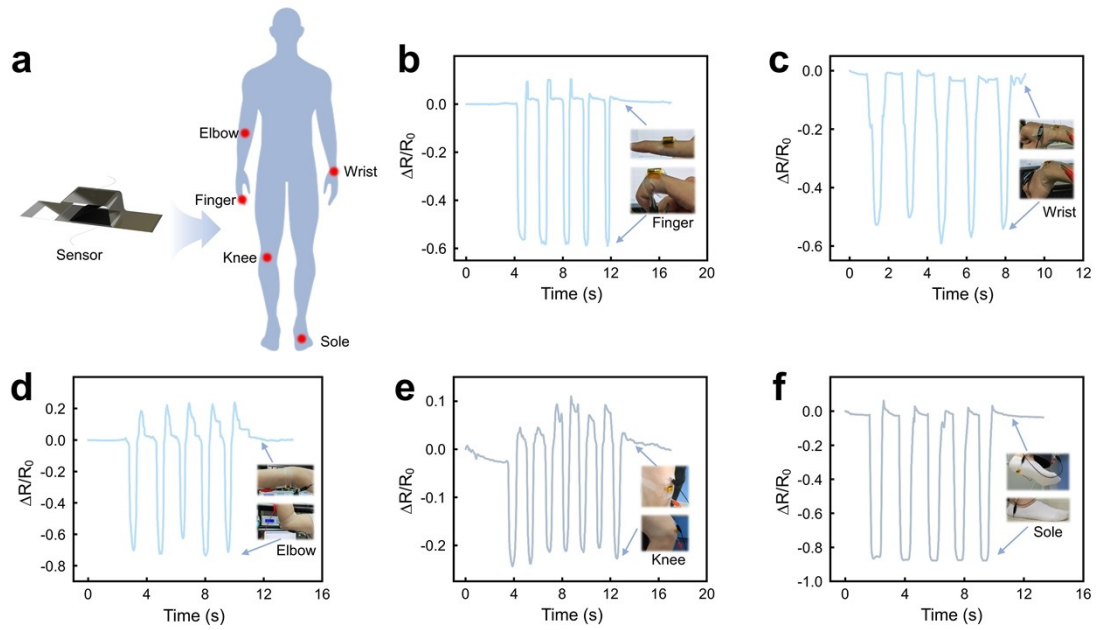
Figure S10. (a) Schematic diagram of a paper-based pressure sensor applied to human activity signal detection. (b) The sensor detects signals of finger bending. (c) The sensor detects the signal of wrist bending. (d) The sensor detects the signal of elbow bending. (e) The sensor detects the signal of knee bending. (f) The sensor detects the signal of the pace of human movement.
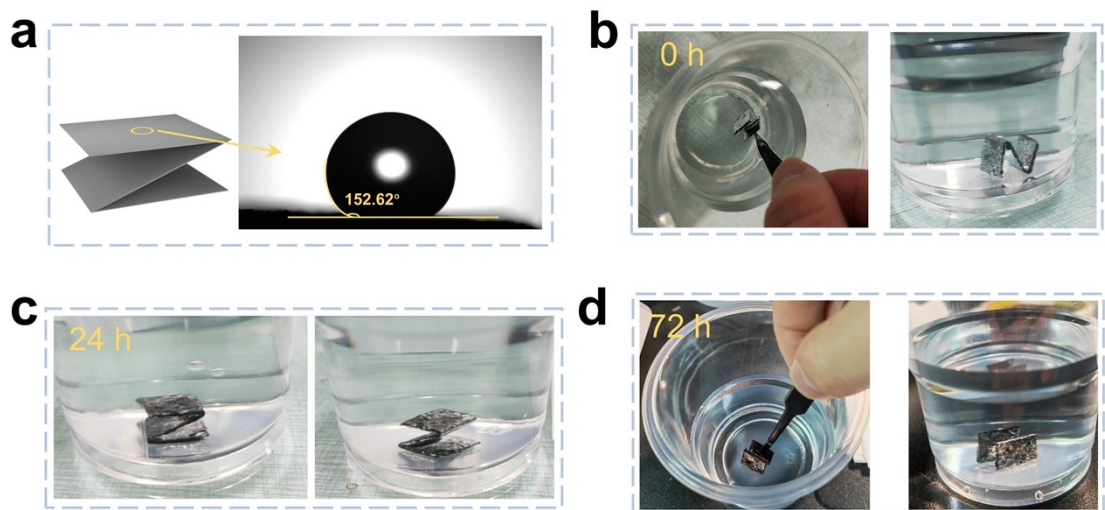
Figure S11. (a) Water contact angle on the surface of the pressure-sensitive layer of a paper-based pressure sensor. (b) Pressure-sensitive layer has just been immersed in water. (c) Pressure-sensitive layer immersed in water for 24 h. (d) Pressure-sensitive layer immersed in water for 72 h.
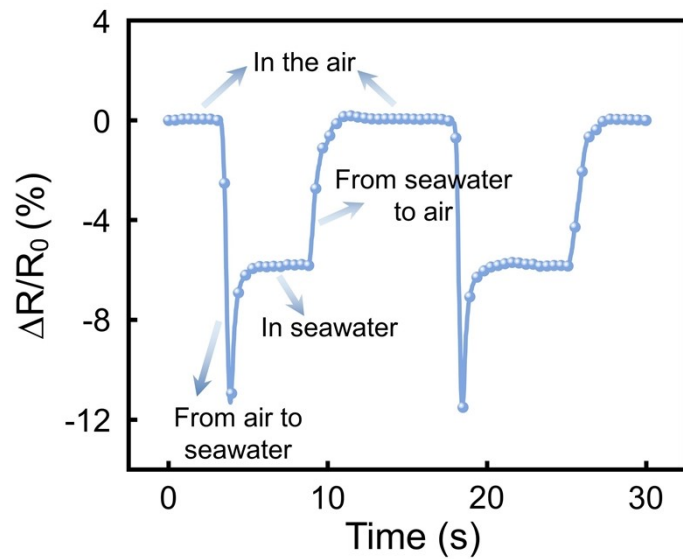
Figure S12. The change in resistance signal of the sensor as it passes from the air into seawater. The concentration of salt water is 35 g/L.

Supplementary Tables

Table S1 Performance comparison of recently reported paper-based pressure sensors

Substrate	Sensitive material	Sensitivity (kPa⁻¹)	Sensing range (kPa)	Cycling stability	Reference
paper	CB/rGO	0.59 at 0-50 kPa 0.09 at 50-250 kPa	0-250	/	1
tissue paper	AgNWs	1.5 at 0.03-30.2 kPa	0-30.2	/	2
tissue paper	MXene	0.55 at 23-982 Pa 3.81 at 982 Pa-10 kPa 2.52 at 10-30 kPa	0-30	10,000	3
copy paper	MWNT	0.014 at 0-70 kPa	0-70	/	4
airlaid paper	MXene	7.65 at 0-3.3 kPa 0.98 at 3.3-12.2 kPa 0.24 at 12.2-50 kPa 0.04 at 50-300 kPa	0-300	1,000	5
Cellulose paper	Polyaniline	2.23 at 5-22 kPa	2-90	800	6
A4 printing paper	carbon ink	0.614 at 0-6 kPa 0.064 at 6-40 kPa	0-50	5,000	7
kraft paper	MWCNTs/CBs	1.4 at 0-0.5 kPa 0.022 at 0.5-23 kPa 4.54×10^{-4} at 23-70 kPa	0-70	1,500	8
paper	SWCNT	5.15 at 0-25 kPa 1.46 at 25-175 kPa 0.42 at 175-450 kPa	0-450	5,000	9
Checkered art paper	MWCNTs/CBs	0.297 at 0-400 Pa 0.111 at 400 Pa-1 kPa	0-1000	5,000	This work

Table S2 Comparison of frequency response with recently reported flexible pressure

sensors

Kind	Material	Maximum frequency response (Hz)	Reference
Piezoresistive	Conductive fabric Silica gel	35	10
Capacitive	PVA/ H_3PO_4 film Epoxy resin/Au	200	11
Piezoresistive	PDMS/Rgo PEN film/AgNPs	250	12
Capacitive	PDMS PVA/ H_3PO_4 film PET/Au	400	13
Piezoelectric	PDMS Epoxy resin PVDF Al electrode	600	14
Piezoresistive	CA-paper MWCNTs/CBs/PDMS Stainless steel framework Cu electrode	1000	This work

Reference

1. H. Liu, H. Xiang, Y. Wang, Z. Li, L. Qian, P. Li, Y. Ma, H. Zhou and W. Huang, *ACS Appl. Mater. Interfaces*, 2019, **11**, 40613–40619.

2. L. Gao, C. Zhu, L. Li, C. Zhang, J. Liu, H.-D. Yu and W. Huang, *ACS Appl. Mater. Interfaces*, 2019, **11**, 25034–25042.

3. Y. Guo, M. Zhong, Z. Fang, P. Wan and G. Yu, *Nano Lett.*, 2019, **19**, 1143–1150.

4. R. Matsukawa, D. Kobayashi, H. Mitsui and T. Ikuno, *Applied Physics Express*, 2020, **13**, 027001.

5. D.-J. Yao, Z. Tang, L. Zhang, Z.-G. Liu, Q.-J. Sun, S.-C. Hu, Q.-X. Liu, X.-G. Tang and J. Ouyang, *J. Mater. Chem. C*, 2021, **9**, 12642–12649.

6. D. Kannichankandy, P. M. Pataniya, S. Narayan, V. Patel, C. K. Sumesh, K. D. Patel, G. K. Solanki and V. M. Pathak, *Synth. Met.*, 2021, **273**, 116697.

7. Z. Duan, Y. Jiang, Q. Huang, S. Wang, Y. Wang, H. Pan, Q. Zhao, G. Xie, X. Du and H. Tai, *Smart Mater. Struct.*, 2021, **30**, 055012.

8. J. Li, Z. Yao, X. Meng, C. Zhang, T. Sun, W. Song, H. Li, J. Zhang, S. Niu, L. Liu, Z. Han and L. Ren, ACS Appl. *Nano Mater.*, 2022, **5**, 18832–18841.

9. C. Zhang, R. Chen, W. Luo, J. Wang, D. Chen, P. Chen, S. Liu, Y. Xie, W. Zhou and T. Luo, *ACS Appl. Mater. Interfaces*, 2023, **15**, 41950–41960.

10. X. Wang, J. Yang, Z. Feng, G. Zhang, J. Qiu, Y. Wu and J. Yang, *ACS Appl. Mater. Interfaces*, 2021, **13**, 55747–55755.

11. N. Bai, L. Wang, Y. Xue, Y. Wang, X. Hou, G. Li, Y. Zhang, M. Cai, L. Zhao, F. Guan, X. Wei and C. F. Guo, *ACS Nano*, 2022, **16**, 4338–4347.

12. H. Yang, R. Fu, X. Shan, X. Lin, Y. Su, X. Jin, W. Du, W. Lv and G. Huang, *Biosens. Bioelectron.*, 2022, **203**, 114028.

13. N. Bai, Y. Xue, S. Chen, L. Shi, J. Shi, Y. Zhang, X. Hou, Y. Cheng, K. Huang, W. Wang, J. Zhang, Y. Liu and C. F. Guo, *Nat. Commun.*, 2023, **14**, 7121.

14. J. Zhang, H. Yao, J. Mo, S. Chen, Y. Xie, S. Ma, R. Chen, T. Luo, W. Ling, L. Qin, Z. Wang and W. Zhou, *Nat. Commun.*, 2022, **13**, 5076.